

Impact of forward bias injection on minority carrier transport in p-type ZnO nanowires

C. Schwarz,¹ E. Flitsiyan,¹ L. Chernyak,^{1,a)} V. Casian,² R. Schneck,² Z. Dashevsky,² S. Chu,³ and J. L. Liu³

¹Department of Physics, University of Central Florida, Orlando, Florida 32816-2385, USA

²Department of Materials Engineering, Ben-Gurion University, Beer-Sheva 84105, Israel

³Department of Electrical Engineering, University of California, Riverside, California 92521, USA

(Received 24 June 2011; accepted 3 August 2011; published online 9 September 2011)

Minority carrier diffusion length in *p*-type Sb-doped ZnO nanowires was measured as a function of temperature and forward bias injection duration. The minority carrier diffusion length displays a thermally activated length increase with the energy of 144 ± 5 meV. The forward bias injection exhibits an increase in diffusion length with the activation energy of 217 ± 20 meV, indicating the possible involvement of a $\text{Sb}_{\text{Zn}}\text{-}2\text{V}_{\text{Zn}}$ acceptor complex. © 2011 American Institute of Physics. [doi:10.1063/1.3633224]

ZnO's fundamental properties, such as its wide-band gap (3.37 eV), high breakdown strength, and large exciton binding energy (60 meV) have generated much interest in this material for use in optoelectronic devices. Coupled with the recent opportunity for ZnO material to be manufactured in the shape of nanowires, greater prospects continue to emerge for ZnO in the field of solid-state electronics. The large surface area of nanowires in combination with the bio-safe characteristics of ZnO makes them attractive candidates for gas, chemical sensing, and biomedical applications.¹⁰ However, achieving good *p*-type conductivity has been a major hurdle for developing ZnO p-n junctions due to the high ionization energies of its potential acceptors. Recent advances in *p*-type doping using larger radii atoms, such as antimony (Sb), have produced ZnO homojunctions with good electrical and optical properties.¹⁴ Studying the diffusion length of minority carriers in ZnO is subsequently important because this property defines the performance of p-n junctions and bipolar devices.

Leading up to this study on forward bias injection in ZnO nanowires, the increase in minority carrier diffusion length, L , through temperature and electron beam irradiation effects have been explored and analyzed both in *p*- and *n*-type GaN and ZnO.^{2-4,12} Due to advances in *p*-type doping, ZnO's unique properties and its advantages over GaN, our focus has been recently shifted to exploring the transport properties in ZnO. Studies show that an increase in L can be induced by temperature and electron beam irradiation for epitaxial *p*-type ZnO doped with Sb.^{2,3} Minority carrier transport has also been recently studied in *p*-type Sb doped ZnO nanowires subjected to electron beam irradiation.⁶ It is also of interest that an increase in minority carrier diffusion length, similar to the electron beam irradiation effect, can be witnessed in *p*-type GaN and ZnO through forward bias electron injection in the epitaxial p-n homo-junctions.^{1,13} In this paper, we report the impact of forward bias electron injection on minority carrier diffusion length in *p*-type Sb-doped ZnO nanowires at variable temperatures.

Experiments reported in this work were carried out on *p*-type Sb-doped nanowire layers. The sample consists of a very thin MgO buffer layer and a 2 μm -thick, undoped *n*-type ZnO epitaxial film grown on a Si (100) substrate by molecular beam epitaxy (MBE) under a growth temperature of 450 °C. The sample was then transferred to a Thermal Scientific quartz tube chemical vapor deposition (CVD), in which the nanowires were grown. During the nanowire growth, the temperature was kept at 600 °C. The result was a *p*-type ZnO nanowire layer measured to be about 5 μm thick. The top surface of nanowire layer was then covered with a silver paste for contacting purposes.

We used the electron beam-induced current (EBIC) technique to extract the minority carrier diffusion length of *p*-type ZnO nanowires. The EBIC technique is dependent on the non-equilibrium carriers generated in semiconductors under the influence of electron beam irradiation and their resulting separation by the built in field of the p-n junction or Schottky diode. As majority carriers are swept away from the region of the p-n junction's built-in field localization, the minority ones instead build up and strengthen the magnitude of the overall electric current (i.e., EBIC). By measuring the EBIC current dependence on the distance from the p-n junction and with the use of Eq. (1), the minority carrier diffusion length, L , can then be extracted from the EBIC line scan.⁴ Using this technique, we measure the minority carrier diffusion length in Sb-doped ZnO nanowire layers (cleaved perpendicular to the growth plane) under various temperatures and with forward bias injection. The EBIC signal was recorded within the nanowire layer, beginning from the *n*-ZnO/*p*-ZnO interface and continuing to the *p*-ZnO nanowire region towards the surface, on a sample cleaved perpendicular to the plane of growth (Fig. 1). The EBIC technique depends explicitly on the space charge region of a sample where the internal electric field exists to separate the carriers. In Fig. 1, one can see the superimposed EBIC line-scan signal following a path of exponential decay in the *p*-type ZnO nanowire region.

All experiments were conducted *in situ* in a Philips XL30 scanning electron microscope (SEM) under an accelerating voltage of 20 kV. A forward bias was applied to the

^{a)}Electronic mail: chernyak@physics.ucf.edu.

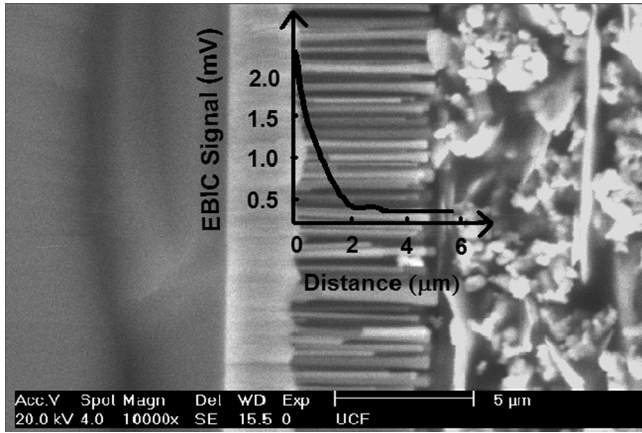


FIG. 1. Secondary electron image of the samples cross section taken perpendicular to the growth plane. From left to right: silicon substrate; n-ZnO film; p-ZnO (nanowire layer); and Ag-epoxy layer (used for a contact). EBIC measurements were taken from the n-ZnO film/p-ZnO nanowire interface. Superimposed: Exponential decay of EBIC signal versus the beam-to-barrier distance.

p-n junction between the *p*-type ZnO nanowires and the *n*-type ZnO film using a Hewlett-Packard 4145A semiconductor parameter analyzer resulting in a current of about 5 mA. After the initial line-scan (24 s), EBIC measurement, and extraction of diffusion length L , the forward bias injection was continued by applying 12 V for up to 600 s in 100 s increments. This was repeated at temperatures adjusted to 25, 45, 55, and 75 °C using an external temperature controller (Gatan). Before measurements were conducted, the sample was freshly cleaved and placed in a vacuum chamber at 2×10^{-6} mBar. Because the electron beam excitation during the measurement period (24 s) was much shorter than the duration of the forward bias injection (hundreds of seconds), the contribution of SEM beam to the electron injection effect as well as to desorption of oxygen and other species (if any) from the nanowires was negligible. A new region was also selected at each temperature and the electron beam was turned off while applying forward bias. Areas for measurements were selected based on absence of visible particles in the region under investigation, as seen from the SEM picture (Fig. 1).

Before performing the experiments on forward bias electron injection in *p*-ZnO nanowires, we first determined the impact of temperature on the minority carrier diffusion length of the sample. The exponential decay of the EBIC signal within the nanowire layer versus distance from the p-n junction interface is fitted to Eq. (1)

$$I = Ad^\alpha \exp\left(-\frac{d}{L}\right), \quad (1)$$

where I is the EBIC signal, A is a constant, d is beam-to-junction distance, and L is the diffusion length. The coefficient, α , responsible for surface recombination, was taken to equal $-1/2$.⁵ The relationship between diffusion length, L , and temperature is displayed in Fig. 2. One can see from this figure that the value of L increases exponentially with temperature increase; this is fitted to Eq. (2)

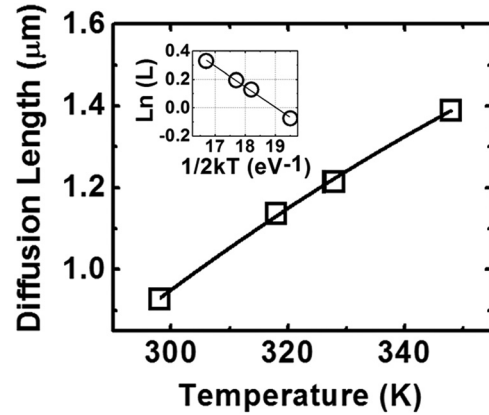


FIG. 2. Dependence of diffusion length on temperature in the nanowire p-ZnO region. Inset: Arrhenius plot for L vs. T dependence resulting in a value for activation energy of 144 ± 5 meV.

$$L = L_0 \sqrt{\exp(-E_a/kT)}, \quad (2)$$

where L_0 is a scaling factor, k is Boltzmann constant, and E_a is the thermal activation energy found to be 144 ± 5 meV (obtained from the Arrhenius plot in the inset of Fig. 2). The latter parameter likely represents carrier delocalization energy and determines the increase of the diffusion length due to the reduction in recombination efficiency.³ Previous photo- and cathodo-luminescence studies on *p*-type ZnO have shown that the recombination route of nonequilibrium carriers involves transitions to a deep, neutral acceptor level (e, A^0).^{9,11} Increasing the temperature of the sample leads to a larger ionization fraction of the acceptors while inhibiting the recombination rate by reducing the concentration of A^0 .

The application of a forward bias to the p-n junction of the sample also resulted in an increase in the minority carrier diffusion length (Fig. 3). However, as the temperature was raised under forward bias, a relative reduction in the diffusion length growth rate can also be observed (Fig. 3). This forward bias injection-induced increase of L suggests that it comes from a similar origin to that of the electron beam irradiation-induced increase.⁶ The effect of electron irradiation on the diffusion length can be attributed to the trapping of non-equilibrium electrons on the neutral acceptor levels ($A^0 + e^- \rightarrow A^-$).

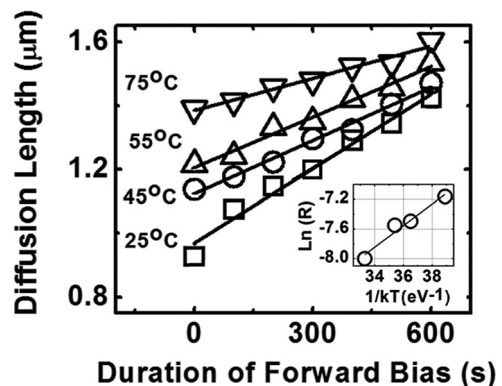


FIG. 3. Linear dependence of the diffusion length on forward bias duration under increasing temperature. The rates, R , of increase of L for each temperature is obtained from the slope. Inset: Arrhenius plot for R vs. T dependence resulting in the activation energy of 217 ± 20 meV.

When the non-equilibrium electron-hole pairs recombine, they involve the levels of neutral acceptors located deep in the band gap. Electron trapping on neutral acceptor levels prohibits the pathway of recombination via these levels and leads to an increase of non-equilibrium minority carrier (electron) lifetime in the conduction band and, in turn, carrier diffusion length. As the excitation proceeds, the concentration of neutral levels decreases, due to electron trapping on them, while the diffusion length steadily rises. Since the presence of Sb has been shown to induce acceptor levels in the band gap far from the valence band edge, it is likely that applying forward bias results in similar effects. This is because the electrons injected into *p*-ZnO become trapped on the Sb-related levels preventing further recombination via these levels and subsequently resulting in the increase of *L*.¹ The dependence of forward bias injection and temperature on the rate *R*, can be quantified by Eq. (3) (Ref. 7)

$$R = R_0 \exp\left(\frac{E_{fbi}}{kT}\right) \exp\left(-\frac{E_a}{2kT}\right), \quad (3)$$

where R_0 is a scaling factor; k is Boltzmann constant; E_a is the thermal activation energy determined from the above-mentioned temperature-dependent *L* measurements (~ 144 meV); E_{fbi} is the activation energy for the forward bias injection-induced effect. Accounting for rates, *R*, at various temperatures, which can be obtained from the dependences of *L* on forward bias injection duration in Fig. 3, E_{fbi} can be calculated from (3) using a linear fitting of $\ln(R)$ vs. $1/kT$, as shown in the inset of Fig. 3. We found E_{fbi} to be 217 ± 20 meV. This is in good agreement with our previous work on *p*-type ZnO nanowires, where the impact of electron beam irradiation on minority carrier transport was studied.⁶

It has been theorized by Limpijumngong *et al.* that the role of acceptors in size-mismatched Sb-impurity doped ZnO is accomplished by a $\text{Sb}_{\text{Zn}}-2\text{V}_{\text{Zn}}$ complex, which is predicted to have an ionization energy of 160 meV.⁸ While our value for activation energy (217 meV) is somewhat larger than the predicted value (160 meV), we can successfully rule out other Sb-related defects such as Sb_o substitutional defects as well as the single vacancy $\text{Sb}_{\text{Zn}}-\text{V}_{\text{Zn}}$ complex, due to their ionization energies being about an order of magnitude larger than our value.⁸ It has also been shown that in

Sb-doped ZnO, acceptor activation energy can vary from about 135 meV ($1.3 \times 10^{18} \text{ cm}^{-3}$) to 212 meV ($1.3 \times 10^{17} \text{ cm}^{-3}$); comparable to the case of ZnO nanowires used in this study) depending on its concentration of majority carriers.⁹

In conclusion, forward bias injection leads to an increase in minority carrier diffusion length in *p*-type Sb-doped ZnO nanowires. Temperature dependent EBIC measurements allow for the estimation of the activation energy of this increase. Using the experimentally obtained values for the activation energy and comparing to known values, the $\text{Sb}_{\text{Zn}}-2\text{V}_{\text{Zn}}$ acceptor-complex was identified as a possible origin for carrier trapping on the deep Sb-related acceptor levels.

The authors would like to thank the National Science Foundation (ECCS Grant No. 0900971) and the U.S.-Israel Binational Science Foundation (Grant No. 2008328) for financial support.

¹O. Lopatiuk-Tirpak, L. Chernyak, L. J. Mandalapu, Z. Yang, J. L. Liu, K. Gartsman, Y. Feldman, and Z. Dashevsky, *Appl. Phys. Lett.* **89**, 142114 (2006).

²L. Chernyak, C. Schwarz, E. Flitsyan, S. Chu, J. L. Liu, and K. Gartsman, *Appl. Phys. Lett.* **92**, 102106 (2008).

³O. Lopatiuk-Tirpak, F. X. Xiu, J. L. Liu, S. Jang, F. Ren, S. J. Pearton, K. Gartsman, Y. Feldman, A. Osinsky, P. Chow, and L. Chernyak, *J. Appl. Phys.* **100**, 086101 (2006).

⁴L. Chernyak, A. Osinsky, H. Temkin, J. W. Yang, Q. Chen, and M. A. Khan, *Appl. Phys. Lett.* **69**, 2531 (1996).

⁵Y. Lin, E. Flitsyan, L. Chernyak, T. Malinauskas, R. Aleksiejunas, K. Jarasiunas, W. Lim, S. J. Pearton, and K. Gartsman, *Appl. Phys. Lett.* **95**, 092101 (2009).

⁶Y. Lin, M. Shatkhin, E. Flitsyan, L. Chernyak, Z. Dashevsky, S. Chu, and J. L. Liu, *J. Appl. Phys.* **109**, 016107 (2011).

⁷O. Lopatiuk, L. Chernyak, A. Osinsky, and J. Q. Xie, *Appl. Phys. Lett.* **87**, 214110 (2005).

⁸S. Limpijumngong, S. B. Zhang, S. H. Wei, and C. H. Park, *Phys. Rev. Lett.* **92**, 155504 (2004).

⁹O. Lopatiuk-Tirpak, W. V. Schoenfeld, L. Chernyak, F. X. Xiu, J. L. Liu, S. Jang, F. Ren, S. J. Pearton, A. Osinsky, and P. Chow, *Appl. Phys. Lett.* **88**, 202110 (2006).

¹⁰Y. W. Heo, D. P. Norton, L. C. Tien, Y. Kwon, B. S. Kang, F. Ren, S. J. Pearton, J. R. LaRoche, *Mater. Sci. Eng. R* **47**, 1 (2004).

¹¹F. X. Xiu, Z. Yang, L. J. Mandalapu, D. T. Zhao, J. L. Liu, and W. P. Beyermann, *Appl. Phys. Lett.* **87**, 152101 (2005).

¹²L. Chernyak, A. Osinsky, V. Fuflyigin, and E. F. Schubert, *Appl. Phys. Lett.* **77**, 875 (2000).

¹³L. Chernyak, G. Nootz, and A. Osinsky, *Electronics Letters*. **37**, 922 (2001).

¹⁴L. Chernyak, A. Osinsky, and A. Schulte, *Solid-State Electron.* **45**, 1687 (2001).